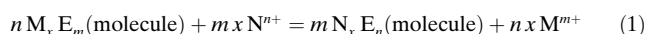


Phosphine-Initiated Cation Exchange for Precisely Tailoring Composition and Properties of Semiconductor Nanostructures: Old Concept, New Applications**

Jing Gui, Muwei Ji, Jiajia Liu, Meng Xu, Jiatao Zhang,* and Hesun Zhu

Abstract: Phosphine-initiated cation exchange is a well-known inorganic chemistry reaction. In this work, different phosphines have been used to modulate the thermodynamic and kinetic parameters of the cation exchange reaction to synthesize complex semiconductor nanostructures. Besides preserving the original shape and size, phosphine-initiated cation exchange reactions show potential to precisely tune the crystallinity and composition of metal/semiconductor core-shell and doped nanocrystals. Furthermore, systematic studies on different phosphines and on the elementary reaction mechanisms have been performed.

Cation exchange, a traditional inorganic reaction,^[1] has become a potential strategy for synthesizing highly monodisperse colloidal nanocrystals (NCs), because it can not only preserve the original shape and size but also control the amount of dopant in semiconductor NCs.^[2–14] Recently, cation exchange has also been demonstrated as an effective way to tailor core-shell, heterodimer hybrid NCs under large lattice mismatches.^[15] Furthermore, compared to the hot-injection method,^[16,17] the cation exchange method can mediate the cation and anion composition as well as the amount of dopant in semiconductor NCs at low temperature, because it can be used to control the thermodynamic and kinetic parameters. However, many cation exchange reactions, as shown in reaction (1), are forbidden, because $\Delta G_{\text{reaction}} > 0$.^[1,3c]



Tertiary phosphines (R_3P) are an important class of ligands because their electronic and steric properties can be altered in a systematic and predictable way over a very wide range by varying the R groups.^[18,19] They can be used to stabilize a variety of transition metal complexes.^[20–23] Therefore, the addition of phosphine agents, which have versatile

coordination abilities to many kinds of transition metals, could induce different cooperation modes between M and N cations and promote reaction (1) ($\Delta G_{\text{reaction}} < 0$).^[19,20]

It is worth mentioning that the Alivisatos group used tributylphosphine (TBP) to mediate cation exchange reactions in ionic nanocrystals and found the complete in situ conversion of silver chalcogenide (Ag_2E , E = chalcogen) NCs to CdE NCs.^[3] Afterwards, TBP has been widely used to synthesize quantum dots with controlled dopant and composition by several groups, such as the Norris, Manna, Klimov, and Ouyang group.^[6,8,24–26] We utilized TBP for the nonepitaxial growth of hybrid metal@semiconductor core-shell and heterodimer NCs under large lattice mismatches.^[15c] However, TBP is easily oxidized to tributylphosphite (TBPO) with flammable and corrosive severity within short time when operated in air, thus leading to the deactivation of cation exchange. There are only a few studies on the flexible chemical thermodynamics and kinetics control by different kinds of phosphine agents. It is very critical because the choice of phosphine will influence the crystallinity and composition of the semiconductor NCs, thus enabling a more flexible tailoring of their optical and electronic properties.

Nonepitaxially grown metal@semiconductor core-shell NCs with monocrystalline semiconductor shell have exhibited flexible plasmon-exciton coupling and enhanced lifetime of excitons.^[15b,27] As a result, the energy of metal nanoparticles can be efficiently utilized by the semiconductor component without undergoing significant nonradiative energy loss. They have potential catalytic and photovoltaic applications due to the nonepitaxial nature of the metal/semiconductor interface associated with low defect density.^[15c,27] Thus, more versatile and facile synthesis of such NCs with well-controlled crystallinity and composition requires further study. Incorporating heterovalent impurities in semiconductor NCs through cation exchange with controlled dopant level and concentration has demonstrated potential optoelectronic applications.^[6,8,24–26] Here, a series of phosphine ligands and other typical organic ligands have been chosen to modulate the thermodynamic and kinetic features of cation exchange in the case of metal@semiconductor core-shell NCs and doped NCs. The mechanism of cation exchange reactions initiated by these phosphine ligands and the control of crystallinity, morphology, and composition of these two types of NCs have been investigated.

Here, we examine the cation exchange between N^{+} in amorphous N_2E (E = chalcogen) nanoparticles (NPs) and M^{2+} (such as Cd^{2+}) ions in solution, as shown in reaction (2)



[*] J. Gui, M. Ji, Dr. J. Liu, Dr. M. Xu, Prof. J. Zhang, Prof. H. Zhu
Research Center of Materials Science
School of Materials Science & Engineering
Beijing Institute of Technology
Beijing 100081 (P. R. China)
E-mail: zhangjt@bit.edu.cn

[**] This work was supported by the National Natural Science Foundation (21322105, 91123001, 51372025, and 91323301), the Research Fund for the Doctoral Program of Higher Education of China (2011101120016), and the Program for New Century Excellent Talents in University (NCET-11-0793). We thank Prof. Min Ouyang of University of Maryland, College Park for helpful discussions.

Supporting information for this article is available on the WWW under <http://dx.doi.org/10.1002/anie.201410053>.

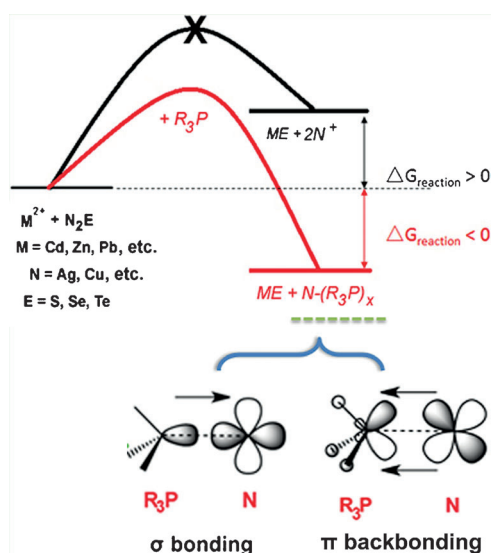


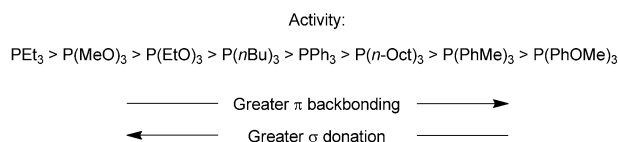
Figure 1. Thermodynamic scheme of the cation exchange reaction initiated by different phosphines or phosphites (R_3P).

and Figure 1. Based on our previous work on Au@ME core-shell NCs under large lattice mismatches,^[15a] many other phosphines besides TBP, have been used to control the thermodynamic and kinetic parameters of reaction (2). Initiated by trace phosphine (R_3P), the crystallinity, morphology, and composition of metal@ME core-shell NCs have been tailored well.

Different phosphine and phosphite agents used in the synthesis of semiconductor shells have been summarized in Table 1. From Table 1 and Figure 1, several conclusions can be drawn. Firstly, the prerequisite to promote cation exchange is the lone-pair electrons of P in phosphines or phosphites. Based on this, the different π -accepting and σ -donating capabilities of the phosphines and phosphites to M and N ions render reaction (2) exothermic ($\Delta G_{\text{reaction}} < 0$).^[18–22] ^{31}P NMR measurements of different phosphines coordinating to Ag^+ and Cd^{2+} and a study of their coordination abilities further prove that reaction (2) is exothermic in principle (see the details in Figure S1 and SI-1 in the Supporting Information, SI).^[23] Therefore, the thermodynamics and kinetics of reaction (2) could be mediated. This explains why TOPO could not promote reaction (2). Secondly, the stronger coordination ability of R_3P to N^+ than to M^{2+} ions enables the in situ conversion of amorphous N_2E nanoparticles to ME NCs. However, pyrazole and imidazole cannot initiate reaction (2), although they show good coordination to many transition metals through their N atoms (see also Table S1). Thirdly, but most importantly, although many kinds of phosphines or phosphites are thermodynamically applicable in reaction (2), the steric effect derived from the carbonyl ligands, such as alkyl and aryl ligands, would influence the kinetics of reaction (2) and therefore the crystallinity and composition of the resulting ME NCs distinctly. One example is the cation exchange from the amorphous Ag_2S nanostructure to form the single-crystalline CdS nanostructure. As illustrated in Table 1, the kinetic activity order is: $\text{PEt}_3 > \text{P}(\text{MeO})_3 > \text{P}(\text{EtO})_3 > \text{P}(n\text{Bu})_3 > \text{PPh}_3 > \text{P}(n\text{-Oct})_3 > \text{P}(\text{PhMe})_3 > \text{P}(\text{PhOMe})_3$. This is

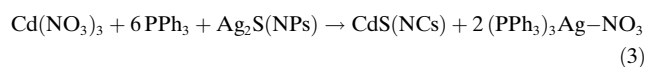
Table 1: Phosphines and phosphites with different alkyl groups and steric properties that were used to promote cation exchange (C.E.) for the synthesis of core-shell metal@semiconductor NCs.

Name	Molecular formula	C.E. reaction conditions
Triethyl phosphine	$(\text{C}_2\text{H}_5)_3\text{P}$	rt, 3–5 min
Trimethyl phosphite	$\text{P}(\text{Et})_3$ $(\text{CH}_3\text{O})_3\text{P}$	rt, 3–5 min
Triethyl phosphite	$\text{P}(\text{MeO})_3$ $(\text{C}_2\text{H}_5\text{O})_3\text{P}$	rt, 5–10 min
Tributyl phosphine (TBP)	$\text{P}(\text{EtO})_3$ $(\text{C}_4\text{H}_9)_3\text{P}$ $\text{P}(n\text{Bu})_3$	rt, 20–30 min (or 30–40 °C, 3–5 min)
Trioctyl phosphine (TOP)	$(\text{C}_8\text{H}_{17})_3\text{P}$ $\text{P}(n\text{-Oct})_3$	40 °C, 30–40 min
Trioctyl phosphine oxide (TOPO)	$(\text{C}_8\text{H}_{17})_3\text{PO}$ $\text{P}(n\text{-OctO})_3$	— ^[a]
Triphenyl phosphine (TPP)	$(\text{C}_6\text{H}_5)_3\text{P}$ PPh_3	30–40 °C, 20–25 min
Tri- <i>p</i> -tolylphosphine	$(\text{C}_7\text{H}_7)_3\text{P}$ $\text{P}(\text{PhMe})_3$	50 °C, 30–40 min
Tris(<i>o</i> -methoxyphenyl) phosphine	$(\text{C}_7\text{H}_7\text{O})_3\text{P}$ $\text{P}(\text{PhOMe})_3$	80 °C > 30 min or 30–40 °C > 1.5 h



[a] No cation exchange observed. rt = room temperature.

almost consistent with their order of σ donation ability and contrary to the π backbonding order. Especially the steric hindrance from carbonyl ligands would distinctly influence the σ donation ability and the chemical kinetics. That is the reason why $\text{P}(\text{PhOMe})_3$ phosphines show low activity in reaction (2). These findings are concordant with Chad Tolman's classic phosphine ligands ordering in terms of their electron-donating ability and steric bulk.^[19] Furthermore, after careful posttreatment of supernatant and ^{31}P NMR characterization (for details see SI-2), we confirmed the existence of $(\text{PPh}_3)_3\text{Ag-NO}_3$. This means that in the case of PPh_3 , reaction (2) happened as follows:



This confirmed the validity of reaction (2) and demonstrated that phosphine promotes cation exchange.

Interestingly, air-stable PPh_3 is a new potential alternative to initiate reaction (2) (see also the analysis in SI-1). Figure 2 shows Au@CdS and Pt@CdS core-shell NCs prepared by reaction (2) initiated with PPh_3 . Following the nonepitaxial growth process we published before,^[15] after the cation exchange from amorphous Ag_2S shell, Au@CdS and Pt@CdS NCs could preserve a thick monocrystalline CdS shell. LRTEM and HRTEM images in Figure 2A–D confirmed their good crystallinity. Especially, as shown in Figure 2D, despite the anisotropic shape of the Pt nanocube, the

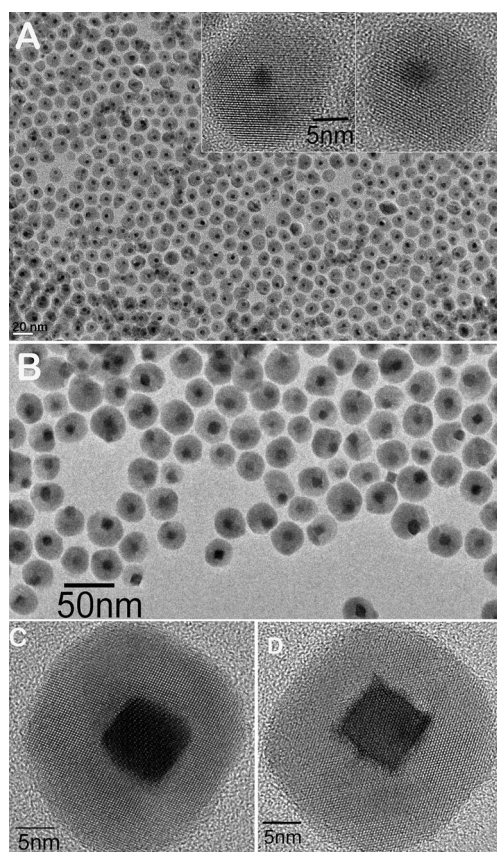


Figure 2. Core-shell metal@semiconductor NCs with thick monocrystalline CdS shell synthesized by PPh_3 initiation under large lattice mismatches: LRTEM and HRTEM images of Au@CdS NCs (A) and Pt@CdS NCs with Pt nanocube core (B–D). Scale bar in (A) = 20 nm.

thick CdS shell has good single-crystallinity. PPh_3 further facilitates to overcome the critical layer thickness limit of heteroepitaxy.^[28] PPh_3 is a “green” choice compared to TBP, because it is sufficiently air-stable to enable reaction (2) under more flexible conditions, such as higher temperature and longer time to facilitate the production of versatile ME NCs.

Moreover, besides crystallization tailoring, PPh_3 could initiate cation exchange to get more complex heterostructures with precise compositional tailoring. Figure 3 A and B showed the LRTEM and HRTEM images of as-prepared Au@CdS_{1-x}Se_x core-shell nanocrystals with ternary single-crystal alloy shell. The S to Se ratio could be tailored (CdS_{0.58}Se_{0.42} and CdS_{0.45}Se_{0.55}, obtained by energy-dispersive X-ray spectroscopy (EDS) elemental analysis) to engineer their bandgaps. The consistent shift of the powder XRD peaks from CdS_{1-x}Se_x shell (Figure 3 C) and the distinct colloid color changing (inset in Figure 3 D) confirmed the homogeneous composition modulation. The strong visible light absorption (550–700 nm; Figure 3 D) due to the surface plasmon resonance (SPR) and exciton coupling in as-prepared Au@CdS_{1-x}Se_x NCs indicated their potential application in photocatalysis and photovoltaics.^[27]

Doped semiconductor NCs with controllable heterovalent impurities have been shown to be an efficient way to control

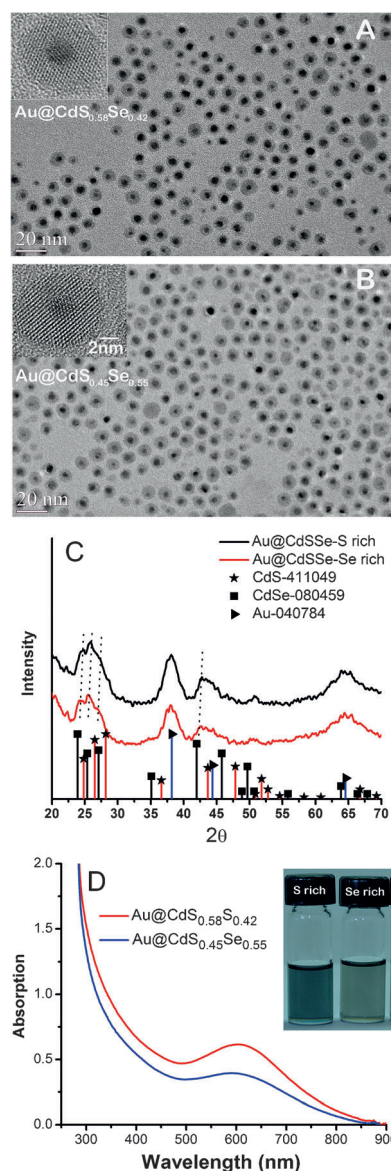


Figure 3. Au@CdS_{1-x}Se_x NCs synthesized by PPh_3 initiation: A–B) LRTEM and HRTEM images of prepared Au@CdS_{0.58}Se_{0.42} NCs and Au@CdS_{0.45}Se_{0.55} NCs. C) Comparison of XRD patterns and D) UV/Vis extinction spectra of Au@CdS_{0.58}Se_{0.42} NCs and Au@CdS_{0.45}Se_{0.55} NCs. Inserted pictures show their colloid color.

the optical, electronic, transport, and magnetic properties.^[29–31] Cation exchange is an effective way to achieve heterovalent doping as shown by many groups, such as the Norris, Banin, and Klimov group.^[14,24,25] Herein, different kinds of phosphine (listed in Table 1) were found to modulate the dopant concentrations through reaction (2). In contrast to the reported methods, firstly, we synthesized highly monodisperse amorphous Ag₂S NPs (Figure 4 B) by treating Ag nanoparticles with an organic sulfur precursor. The amorphous state is helpful for ion motion inside and further cation exchange to achieve a single-crystalline matrix.^[32] Secondly, through cation exchange with Cd²⁺ promoted by different phosphines, single-crystalline CdS NCs could be synthesized successfully. Figure 4 A and C shows the TEM images of CdS

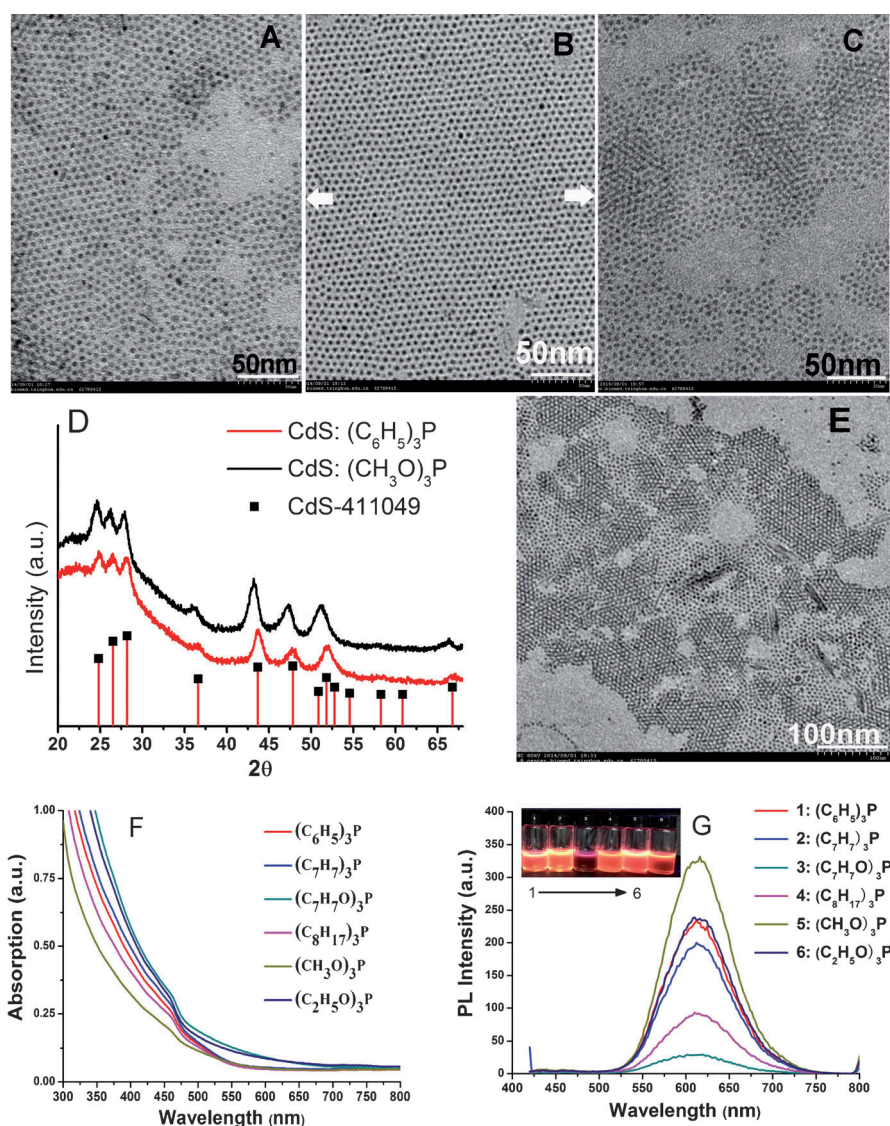


Figure 4. Cation exchange enabled the tailoring of the synthesis and optical properties of Ag-doped CdS NCs: A) HRTEM image of as-prepared CdS NCs by initiation with $(\text{CH}_3\text{O})_3\text{P}$. B) Amorphous Ag_2S nanoparticles. C) CdS NCs obtained by initiation with $(\text{C}_6\text{H}_5)_3\text{P}$. D) XRD patterns of CdS NCs in (A) and (C). E) Self-assembly of CdS NCs synthesized by initiation with $(\text{C}_7\text{H}_7)_3\text{P}$. F–G) Comparison of UV/Vis absorption spectra and related fluorescence spectra ($\lambda_{\text{ex}} = 400 \text{ nm}$) of CdS NCs obtained by using different phosphines or phosphites under the same reaction conditions. The inset is a digital photograph of fluorescence under irradiation with a 365 nm ultraviolet lamp.

NCs synthesized with $(\text{CH}_3\text{O})_3\text{P}$ and $(\text{C}_6\text{H}_5)_3\text{P}$, respectively. XRD patterns in Figure 4D confirmed their good crystallinity. Using $(\text{C}_7\text{H}_7)_3\text{P}$ to initiate cation exchange, the as-prepared CdS NCs have a high monodispersity and show uniform self-assembly to a superlattice (Figure 4E). Figure S2 also shows monodisperse CdS NCs synthesized with $\text{P}(\text{EtO})_3$, $\text{P}(\text{nBu})_3$, $\text{P}(\text{n-Oct})_3$, and $\text{P}(\text{PhOMe})_3$. Especially, the as-prepared CdS NCs obtained with these phosphines exhibited novel optical properties. As shown in Figure 4F and G, there are almost no exciton absorption peaks in their UV/Vis absorption spectra, although the CdS NCs had a high monodispersity. Compared to undoped CdS NCs of the same size and shape,^[16] these CdS NCs emitted red fluorescence. The

luminescence arising from exciton emission ($\approx 460 \text{ nm}$) was very weak. The luminescence peaks at 550–700 nm were stronger. This stronger emission should result from the Ag dopant impurity induced shallow defect energy level.^[33] Furthermore, using different kinds of phosphines in reaction (2), different reaction thermodynamics and kinetics are obtained that lead to different concentrations of the Ag residue. Thus, the dopant luminescence intensity could be mediated more flexibly (see also the fluorescence spectra comparison for using the same phosphine under different reaction time and temperatures in Figure S3A and the fluorescence comparison for using different phosphines under the same reaction time and temperature in Figure S3B). Thus, as-prepared CdS NCs will have potential bioimaging and biosensing applications due to their large Stokes shift and flexible dopant luminescence intensity regulation.^[34,35] More precise control of Ag dopant concentration, position, and resulting shallow energy level will be further studied. Nevertheless, this study provided a new way to synthesize doped semiconductor NCs with precise control of dopant-related optoelectronic properties.

In conclusion, by using different phosphines, the traditional cation exchange reaction could be used to synthesize semiconductor nanostructures with a more flexible degree of control of their crystallinity, composition, morphology, and related optical properties, especially for metal/semiconductor core-shell nanocrystals and doped nanocrystals. This is mainly due to the fact that different phosphines could enable flexible ther-

modynamic and kinetic control of the cation exchange because of their different coordination capability to transition metal ions and the steric effect derived from carbonyl ligands. PPh_3 was found to be a potential alternative. Due to the versatility of phosphine-initiated cation exchange, this approach should offer a general and constructive method to create a wide range of complex semiconductor nanostructures with desired multifunctionality.

Received: October 13, 2014

Revised: December 1, 2014

Published online: January 29, 2015

Keywords: cation exchange · core-shell nanocrystals · doped nanocrystals · phosphine ligands · semiconductors

- [1] J. L. Pauley, *J. Am. Chem. Soc.* **1954**, 76, 1422.
- [2] A. Mews, A. Eychmüller, M. Giersig, D. Schooss, H. Weller, *J. Phys. Chem.* **1994**, 98, 934.
- [3] a) D. H. Son, S. M. Hughes, Y. Yin, A. P. Alivisatos, *Science* **2004**, 306, 1009; b) B. J. Beberwyck, A. P. Alivisatos, *J. Am. Chem. Soc.* **2012**, 134, 19977; c) B. J. Beberwyck, Y. Surendranath, A. P. Alivisatos, *J. Phys. Chem. C* **2013**, 117, 19759.
- [4] S. Gupta, S. V. Kershaw, A. L. Rogach, *Adv. Mater.* **2013**, 25, 6923.
- [5] a) X. Wu, Y. Yu, Y. Liu, Y. Xu, C. Liu, B. Zhang, *Angew. Chem. Int. Ed.* **2012**, 51, 3211; *Angew. Chem.* **2012**, 124, 3265; b) Y. Yu, J. Zhang, X. Wu, W. Zhao, B. Zhang, *Angew. Chem. Int. Ed.* **2012**, 51, 897; *Angew. Chem.* **2012**, 124, 921.
- [6] a) H. Li, M. Zanella, A. Genovese, M. Povia, A. Falqui, C. Giannini, L. Manna, *Nano Lett.* **2011**, 11, 4964; b) H. Li, R. Brescia, R. Krahne, G. Bertoni, M. J. P. Alcocer, C. D. Andrea, F. Scotognella, F. Tassone, M. Zanella, M. D. Giorgi, L. Manna, *ACS Nano* **2012**, 6, 1637; c) H. Li, R. Brescia, M. Povia, M. Prato, G. Bertoni, L. Manna, I. Moreels, *J. Am. Chem. Soc.* **2013**, 135, 12270; d) K. Miszta, D. Dorfs, A. Genovese, M. R. Kim, L. Manna, *ACS Nano* **2011**, 5, 7176.
- [7] A. M. Smith, S. M. Nie, *J. Am. Chem. Soc.* **2011**, 133, 24.
- [8] J. M. Pietryga, D. J. Werder, D. J. Williams, J. L. Casson, R. D. Schaller, V. I. Klimov, J. A. Hollingsworth, *J. Am. Chem. Soc.* **2008**, 130, 4879.
- [9] P. H. C. Camargo, Y. H. Lee, U. Jeong, Z. Zou, Y. N. Xia, *Langmuir* **2007**, 23, 2985.
- [10] C. Chen, X. He, L. Gao, N. Ma, *ACS Appl. Mater. Interfaces* **2013**, 5, 1149.
- [11] C. Dong, F. C. J. M. V. Veggel, *ACS Nano* **2009**, 3, 123.
- [12] M. Sytnyk, R. Kirchschrager, M. I. Bodnarchuk, D. Prietzhofer, D. Kriegner, H. Enser, J. Stangl, P. Bauer, M. Voith, A. W. Hassel, F. Krumeich, F. Ludwig, A. Meingast, G. Kothleitner, M. V. Kovalenko, W. Heiss, *Nano Lett.* **2013**, 13, 586.
- [13] L. Dloczik, R. Könenkamp, *Nano Lett.* **2003**, 3, 651.
- [14] D. Mocatta, C. G. Guy, J. Schattner, O. Millo, E. Rabani, U. Banin, *Science* **2011**, 332, 77.
- [15] a) J. Zhang, Y. Tang, K. Lee, M. Ouyang, *Science* **2010**, 327, 1634; b) J. Zhang, Y. Tang, K. Lee, M. Ouyang, *Nature* **2010**, 466, 91; c) Q. Zhao, M. Ji, H. Qian, B. Dai, L. Weng, J. Gui, J. Zhang, M. Ouyang, H. Zhu, *Adv. Mater.* **2014**, 26, 1387.
- [16] D. V. Talapin, J. Lee, M. V. Kovalenko, E. V. Shevchenko, *Chem. Rev.* **2010**, 110, 389.
- [17] C. B. Murray, D. J. Norris, M. G. Bawendi, *J. Am. Chem. Soc.* **1993**, 115, 8706.
- [18] P. C. J. Kamer, P. Leeuwen, *Phosphorus(III) ligands in homogeneous catalysis: design and synthesis*, Wiley, Hoboken, **2012**.
- [19] C. Tolman, *Chem. Rev.* **1977**, 77, 313 (Dupont Chemicals).
- [20] D. Fenske, J. Ohmer, J. Hachgenei, K. Merzweiler, *Angew. Chem. Int. Ed. Engl.* **1988**, 27, 1277; *Angew. Chem.* **1988**, 100, 1300.
- [21] G. Schmid, *Nanoparticles: From Theory to Application* (Eds.: A. Eychmüller, U. Banin, S. Dehnen, A. Eichhöfer, J. F. Corrigan, D. Fenske), Wiley-VCH, Weinheim, **2004**, chap. 3a, p. 50.
- [22] M. Tsutsui, M. Hancock, J. Ariyoshi, M. N. Levy, *Angew. Chem. Int. Ed. Engl.* **1969**, 8, 410; *Angew. Chem.* **1969**, 81, 453.
- [23] F. Xu, L. Weng, L. Sun, Z. Zhang, Z. Zhou, *Organometallics* **2000**, 19, 2658.
- [24] A. Sahu, M. S. Kang, A. Kompch, C. Notthoff, A. W. Wills, D. Deng, M. Winterer, C. D. Frisbie, D. J. Norris, *Nano Lett.* **2012**, 12, 2587.
- [25] S. Brovelli, C. Galland, R. Viswanatha, V. I. Klimov, *Nano Lett.* **2012**, 12, 4372.
- [26] L. Weng, H. Zhang, A. O. Govorov, M. Ouyang, *Nat. Commun.* **2014**, 5, 4792.
- [27] S. Lambright, E. Butaeva, N. Razgoniaeva, T. Hopkins, B. Smith, D. Perera, J. Corbin, E. Khon, R. Thomas, P. Moroz, A. Mereshchenko, A. Tarnovsky, M. Zamkov, *ACS Nano* **2014**, 8, 352.
- [28] J. E. Ayers, *Heteroepitaxy of Semiconductors: Theory, Growth and Characterization*, CRC, New York, **2007**.
- [29] S. Jana, G. Manna, B. B. Srivastava, N. Pradhan, *Small* **2013**, 9, 3753.
- [30] Z. Zhang, D. Li, R. G. Xie, W. Yang, *Angew. Chem. Int. Ed.* **2013**, 52, 5052; *Angew. Chem.* **2013**, 125, 5156.
- [31] M. S. Kang, A. Sahu, C. D. Frisbie, D. J. Norris, *Adv. Mater.* **2013**, 25, 725.
- [32] C. Anson, A. Eichhöfer, I. Issac, D. Fenske, O. Fuhr, P. Sevilano, C. Persau, D. Stalke, J. Zhang, *Angew. Chem. Int. Ed.* **2008**, 47, 1326; *Angew. Chem.* **2008**, 120, 1346.
- [33] P. Peng, B. Sadtler, A. P. Alivisatos, R. J. Saykally, *J. Phys. Chem. C* **2010**, 114, 5879.
- [34] J. Yao, S. Schachermeier, Y. D. Yin, W. Zhong, *Anal. Chem.* **2011**, 83, 402.
- [35] P. Wu, X. P. Yan, *Chem. Soc. Rev.* **2013**, 42, 5489.